

Optical tweezers escape forces

Ann A. M. Bui¹, Alexander B. Stilgoe¹, Nima Khatibzadeh², Timo A. Nieminen¹, Halina Rubinsztein-Dunlop¹ and Michael W. Berns^{2,3}

¹School of Mathematics and Physics, The University of Queensland, Brisbane QLD 4072, Australia

²Beckman Laser Institute and Medical Clinic, University of California, Irvine, 92912, USA

³Institute of Engineering in Medicine, University of California, San Diego, 92093, USA

ABSTRACT

With suitable calibration, optical tweezers can be used to measure forces. If the maximum force that can be exerted is of interest, calibration can be performed using viscous drag to remove a particle from the trap, typically by moving the stage. The stage velocity required to remove the particle then gives the escape force. However, the escape force can vary by up to 30% or more, depending on the particle trajectory. This can have significant quantitative impact on measurements. We describe the variation of escape force and escape trajectory, using both experimental measurements and simulations, and discuss implications for experimental measurement of forces.

Keywords: Optical tweezers, optical force, calibration

1. INTRODUCTION

Since the development of optical tweezers in 1986,¹ they have been widely used for quantitative force measurements, especially in biophysics, typically trapping a small bead as a probe particle. However, to measure forces, the trap needs to first be calibrated. A common calibration method is to find the spring constant of the bead in the trap. For small displacements of the bead from equilibrium position, there is a simple linear relation between force and position, and trap strength. However, the spring constant does not describe the behaviour of the trap when the trapped particle is far from the equilibrium position.

Another mode of measuring forces using optical tweezers is to use the force required to remove a particle from the trap. For a given trapping power, this can tell us whether or not the force we are measuring is greater than or smaller than this escape force. Furthermore, we can find the smallest power that can hold the particle in the trap (or, equivalently, largest power at which the particle escapes), and use the linear relationship between force and power to determine the force. This allows relatively large forces to be measured. Since the escape occurs beyond the linear region of the trap, the spring constant calibration described above is not adequate.

The escape force can be measured by applying a steadily increasing force until the particle escapes from the trap. The most common way to apply such a force is to move the stage, resulting in fluid flow past the trapped particle. This results in a viscous drag force, proportional to the stage velocity. Since the flow is at very low Reynolds numbers, the drag is given by Stokes' formula,

$$\mathbf{F}_{\text{drag}} = -6\pi\eta a\mathbf{v}, \quad (1)$$

where a is the radius of the trapped particle, η is the viscosity of the surrounding fluid, and the flow velocity is \mathbf{v} . It is usual and convenient to describe the force by the normalised force efficiency, \mathbf{Q} , such that

$$\mathbf{Q} = \frac{c}{nP}\mathbf{F} \quad \Rightarrow \quad \mathbf{F} = \frac{n\mathbf{Q}}{c}P \quad (2)$$

Further author information: (Send correspondence to T.A.N.)

T.A.N.: E-mail: timo@physics.uq.edu.au

where \mathbf{F} is the trapping force, n is the refractive index of the suspending medium, P the transmitted optical power, and c the speed of light in vacuum.

However, the escape force depends on the path taken by the particle during its escape. This is because the vertical (i.e., axial) component of the optical force ceases to be zero when we displace the particle horizontally from the equilibrium.^{2,3} Provided the particle has sufficient time to move to the new axial equilibrium position, the particle will follow a curved path in its escape. If the particle is moved quickly enough horizontally, it will not reach this vertical equilibrium position, and will follow a different path. In the extreme limit of fast escape, the escape path will be a straight horizontal trajectory. The trajectories for very slow and very fast escapes are shown in figure 1. For intermediate escape speeds, the escape trajectory will lie between these limits.

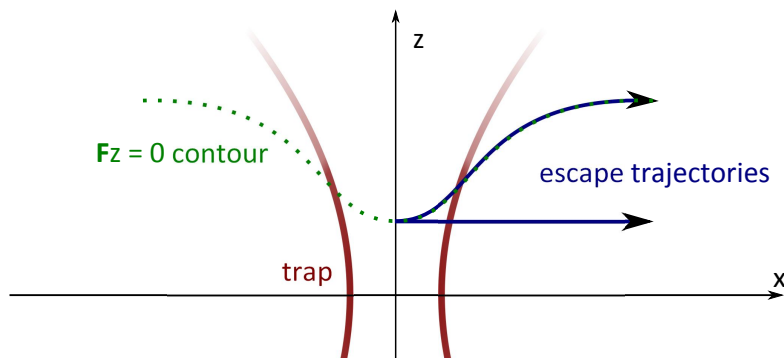


Figure 1. A particle with the trapping beam in the z -direction and an escape force applied in the x -direction. The assumed trajectory of a particle as it escapes from a trap is goes straight out of the trap parallel to the x -axis, which occurs when the trapping force is applied to the particle quickly. However, when the escape force is applied slowly, the particle escapes along the contour where the trapping axial trapping force is zero.

2. METHOD

The experiment was performed by two different laboratories. One experimental component of this work was performed with a standard-type optical tweezers configuration with computerised stage control. The optical tweezers driving laser is a polarisation stabilised Yt. doped fibre laser (YLM-5-LP, IPG Photonics) with output wavelength of 1070 nm. After some relay steering optics the laser input overfills a N.A. = 1.3 microscope objective (Zeiss Plan Fluor EC100). The 4.5 micron diameter polystyrene bead solutions (Polysciences Pty. Ltd.) were held on a piezo electric stage (PI-563.3CD, Physik Instrumente) operating in closed-loop mode and controlled with a PCI card (PI-751E, Physik Instrumente). The drive force is simulated in the apparatus by a single accelerating position ramp creating an increasing viscous drag. Our criteria of escape is the point at which the apparent particle velocity begins to change to match that of the stage. This will usually correspond to the point in the force field where there is a rapid fall from the peak restoring force.

In the other optical tweezers system, a continuous wave 1070 nm wavelength ytterbium fiber laser (PYL-20M, IPG Photonics) is focussed through a high numerical aperture (N.A. = 1.4) oil immersion, Phase III, 100 \times objective (Zeiss Plan-Apochromat). However it has been demonstrated that due to the series of optical aberrations the effective numerical aperture was of the order of 0.8. A microstepper-motor driven stage for inverted microscopes (Ludl Electronic Products, BioPrecision2, NY, USA) was used to provide controlled transverse motions in x and y directions. The stage was driven by the LabView (LabView 8.5.1, National Instruments, TX, USA) based RoboLase III system software through which the stage could be controlled and driven in x and y directions at given velocities over desired distances with a minimum movement resolution of 200nm.

Correlated stage/camera estimate of particle position with time and velocity show that the fluid motion and particle motion can be accurately measured independently of each other. There is some small deviation between the camera and stage because of uncertainty associated with the time that the stage reports its position (up to 10ms, most likely due to polling in the PID loop). Taking the derivative usually magnifies the effect of

uncertainty in measurements. To get a more accurate velocity the data was averaged over 40 time steps. This allows us to unambiguously show the slope of the velocity and hence the acceleration of the stage.

Simulations of the escape of spheres were performed. Optical forces were calculated using our Optical Tweezers Toolbox.^{4,5} During the simulation, we record the total force acting on the particle as well the velocity and position of the particle and stage and the corresponding time. From the recorded positions, the escape velocity and hence the escape force could be calculated as in experiment. The escape force was taken to be the magnitude of the greatest optical force acting on the particle in the direction of stage movement.

3. RESULTS

One of our runs for the trapped particle is shown in figure 2. Figure 2a) shows the position trace of the particle. In the optically trapped region the displacement in the optical trap is roughly proportional to the velocity, consistent with the simple spring model. At escape the particle begins to move with the stage. Figure 2b) shows the derivative of the data displayed in a). It is clear to determine the point of escape using the velocity data. This is because the acceleration in this regime is much smaller than the velocity of the stage. The particle rapidly accelerates to the new velocity as it passes the peak restoring force in the optical trap. Thus we can employ a linear fit routine to fit the near constant velocity within the trap and the linear increase occurring at particle escape.

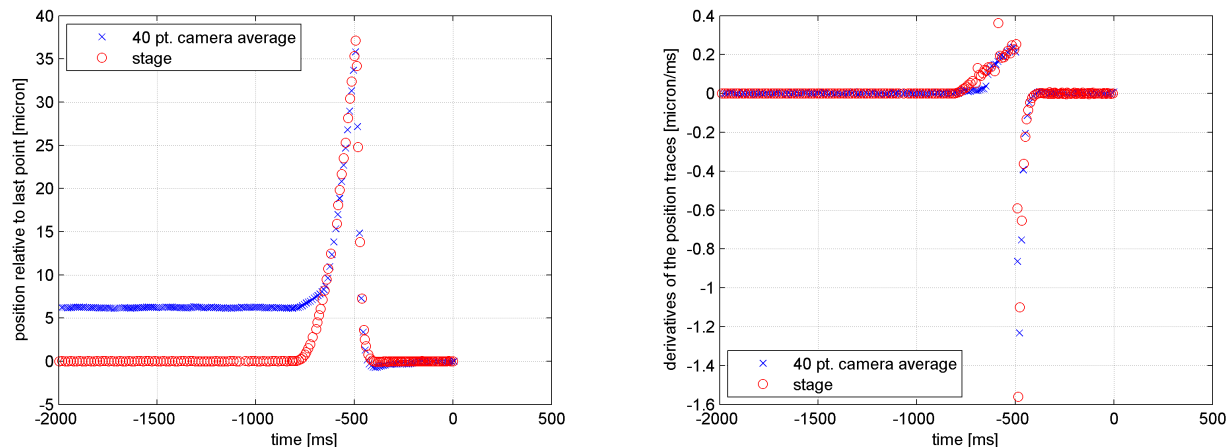


Figure 2. a) Whilst a micro particle is trapped external forces result in an offset in position, must like a velocity. The point of the plot where the particle begins to move with the stage is considered to be the point of escape. b) The derivative clearly shows the time of escape. Whilst in the trap the velocity of the particle relative to the optical traps is close to zero, once its lost it jumps to the velocity of the stage, giving rise to a step in the derivative.

There were escape simulations to match the initial conditions of the two sets of experiments. One set was $4.5\mu\text{m}$ polystyrene sphere in water with stage acceleration of $8.33 \times 10^{-5} \text{ ms}^{-2}$ for low trapping powers of 5-10 mW. The other set was for $4.5\mu\text{m}$ and $10\mu\text{m}$ polystyrene spheres in methyl cellulose solution with viscosities of 1, 3 and 7 cP, with stage acceleration of $1 \times 10^{-6} \text{ ms}^{-2}$ and greater trapping powers of 25-60 mW.

Not shown directly with the experimental conditions, we can explore the escape behaviour of the particle over a range of stage accelerations spanning several orders of magnitude. Figure 3 show the escape trajectory of a $4.5\mu\text{m}$ polystyrene bead on top of an optical force map as it escapes from a 4 mW trap. The different trajectories correspond to different accelerations used to move the stage from rest. For smaller accelerations, the particle does not escape from the trap directly in the direction of the stage, but is pushed away in the direction of beam propagation, following the valley of low Q_z . This results in a different location of escape, corresponding to a lower escape velocity required to escape, and thus a lower escape force measurement.

Figure 4 shows the Q_z corresponding to the trajectories of Figure 3. The lower accelerations correspond to escape forces that were measured during the experiment, but underestimate the greatest possible force that

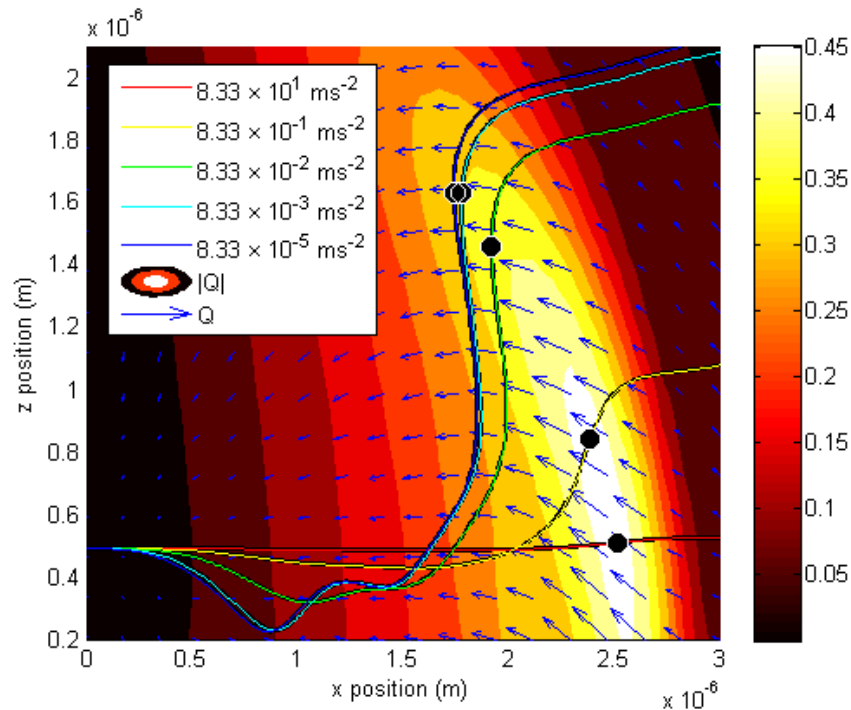


Figure 3. Simulated escape trajectories The vector field shows the direction of force. The different trajectories show the different paths taken by the sphere as it leaves the trap for different accelerations.

the trap can exert. As the acceleration increases, the curve approaches the expected force-position curve which corresponds to the escape trajectory being long the transverse axis.

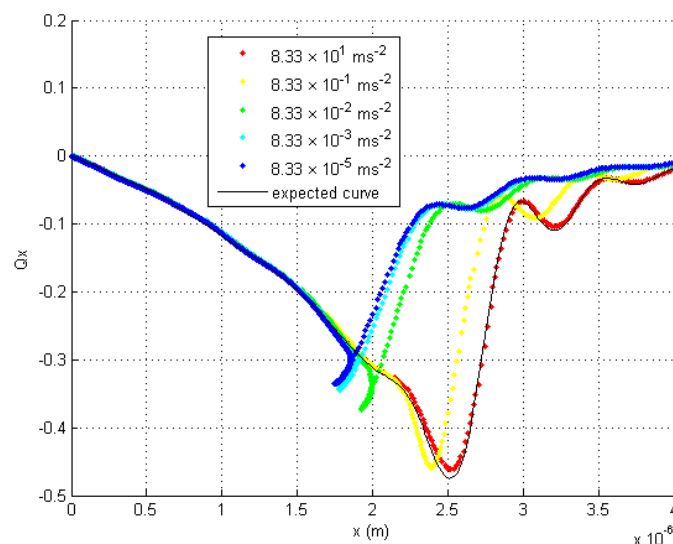


Figure 4. This compares our expected force-position curve against the actual force (in that direction) exerted in the particle. We see that with great acceleration, we follow the expected curve (resulting from movement straight out of the trap). Low acceleration results in a maximum force earlier along the trajectory, and a smaller escape Q

Figure 5 compares experimental measurements with simulations. Measurements were made with fluids of different viscosities to give a higher range of drag forces. In figure 5 we can see that a constant escape Q is not obtained. Since we can perform simulations over a much wider range of accelerations and powers possible with our experiments, the simulations provide an ideal tool for exploring the power and acceleration dependence of the “measured” escape Q . In order to allow a simple and uniform comparison, we plot the simulated escape Q against the acceleration/power², in figure 6.

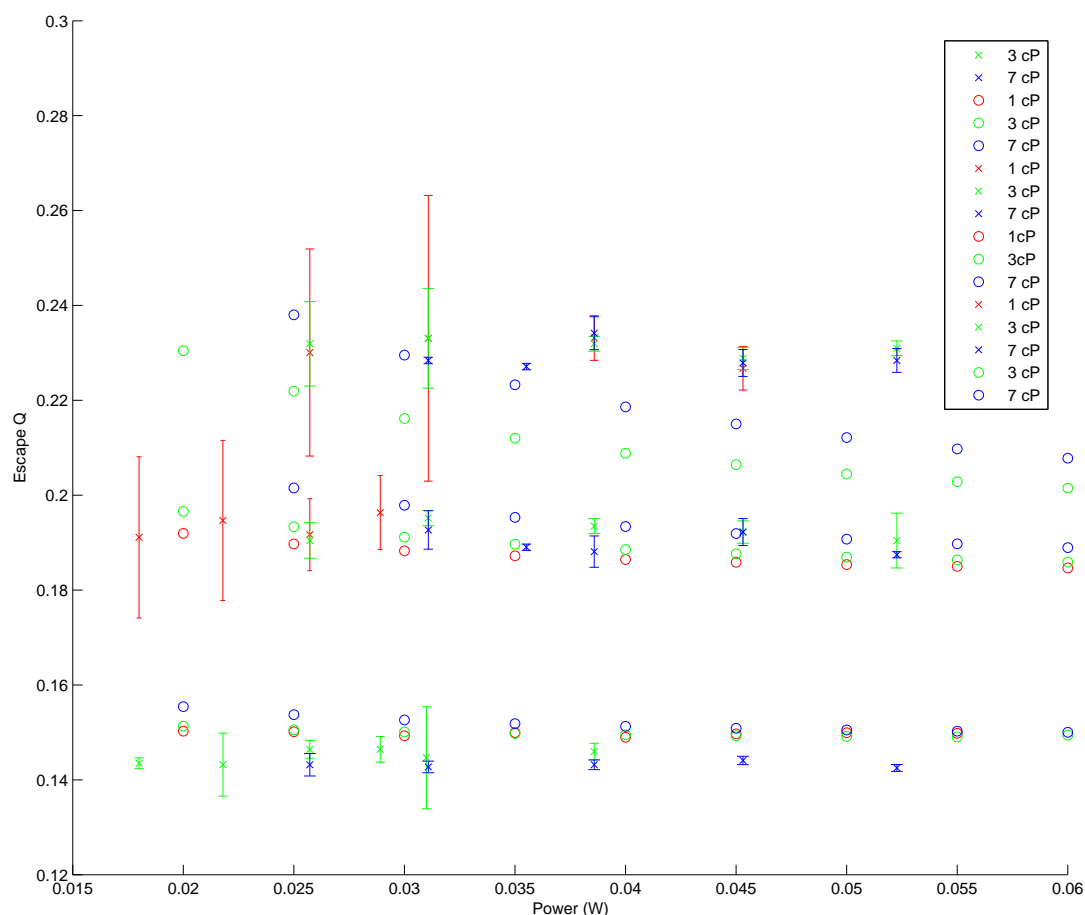


Figure 5. Experimental measurements of escape Q $4.5\mu\text{m}$ and $10\mu\text{m}$ polystyrene sphere with the matching simulation. Escape Q is shown as a function of trapping power over a range of viscosities; the different viscosities give experimental access to a wider range of drag forces. The variation in Q is a result of the lower tail regions of the different curves in figure 6 being at different values of Q .

In figure 6, we see distinct low Q and high Q regimes. These correspond to the escape on a trajectory close to the curved axial equilibrium path (low Q) and escape along an approximately horizontal trajectory. The transition between the two regimes consists of the intermediate trajectories. In the experiments shown in figure 5, the accelerations and powers were such that all measurements were in the low Q regime. Where then did the variation with power come from? In figure 6, especially for the $10\mu\text{m}$, the curves for different powers do not overlap even in the high and low Q regimes. As different powers are used in the experimental measurements of escape, the different low- Q values of these curves are measured.

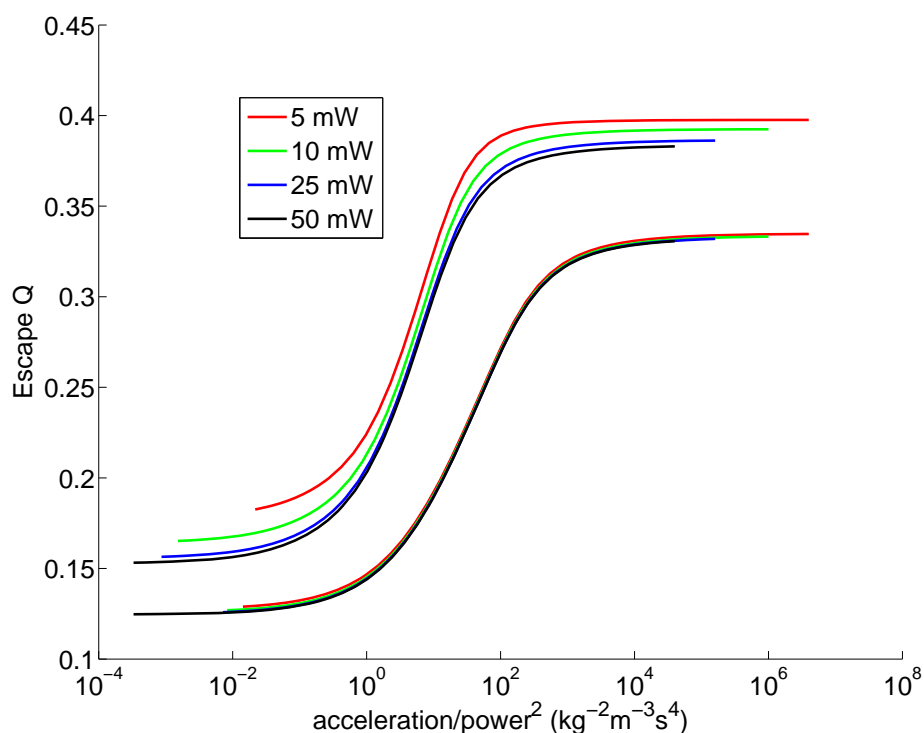


Figure 6. This shows that there are two regions of Q —a high Q for high accelerations and a low Q for low accelerations. The upper set of curves is for $10\mu\text{m}$ spheres, and the lower set is for $4.5\mu\text{m}$ spheres. Changing the power changes when this transition occurs with respect to acceleration. Scaling by the square of the power shows the same behaviour for different trapping powers. The slight non-overlap in the curves for different trapping powers at the lower tail results in the variation in the escape trapping powers seen in figure 5.

4. DISCUSSION AND CONCLUSION

We have shown that the driven escape of spherical particles from optical traps does not necessarily represent the maximum confinement in the horizontal direction. The effect is due to the changing vertical (i.e., axial) equilibrium location. We have also shown that the trajectory of escape and hence the measurement of escape force depends on the rate at which the drive force changes. The temporal power law relationship of escape trajectories is linked to the total external force and can be accounted for by an order-of-magnitude estimate. This effect should be considered when operating near the limits of optical confinement as well.

If the escape force is used to find the escape force of a sphere, then that escape force is taken to be the force of that trap on a similar particle, escaping under similar conditions, then that initial escape force measurement provides a reliable calibration for the trap. The importance is that the escape force is exactly that: the force required to remove a particle from the trap. It does not give a value on the greatest force that could possibly be exerted on a particle.²

A large variation in the escape Q is possible, with more than a factor of two difference between the highest and lowest values of the escape Q shown in figure 6. However, for a strong trap (which is what is likely to be used to measure the high forces requiring measurement by escape force), very high accelerations are needed to reach the high- Q regime. Therefore, one would typically be operating in the low- Q regime. However, even within that low- Q regime, the escape Q is still slightly power dependent. This deviation was shown in figures 5 and 6. Since it is expected that the power will be varied in order to find the power required to keep the particle within the trap against the force acting to remove it, this variation with power can be important. For large particles, this can result in variations in escape Q of up to 30%.

A simple approach is to accept this variation as an uncertainty in the escape force. A more complete approach is to perform the calibration measurements with a range of powers and accelerations, in order to obtain a better understanding of the escape process for the trap in question. Such measurements can be supported by simulations of escape. If the measurements and simulations show that, for the particle size in question, in the trap being calibrated, that the variation with power is small (e.g., as for the $4.5\mu\text{m}$ spheres in figure 6), then one can be confident in having a consistent and robust calibration for the powers in use. If, instead, one finds the escape Q changes significantly, then measurement of the velocity during the escape will allow the escape Q to be estimated more accurately for a given observed escape.

REFERENCES

1. A. Ashkin, J. M. Dziedzic, J. E. Bjorkholm, and S. Chu, "Observation of a single-beam gradient force optical trap for dielectric particles," *Optics Letters* **11**, pp. 288–290, 1986.
2. Z. Gong, Z. Wang, Y. Li, L. Lou, and S. Xu, "Axial deviation of an optically trapped particle in trapping force calibration using the drag force method," *Optics Communications* **273**, pp. 37–42, 2007.
3. A. B. Stilgoe, T. A. Nieminen, G. Knöner, N. R. Heckenberg, and H. Rubinsztein-Dunlop, "The effect of Mie resonances on trapping in optical tweezers," *Optics Express* **16**(19), pp. 15039–15051, 2008.
4. T. A. Nieminen, V. L. Y. Loke, A. B. Stilgoe, G. Knöner, A. M. Brańczyk, N. R. Heckenberg, and H. Rubinsztein-Dunlop, "Optical tweezers computational toolbox," *Journal of Optics A: Pure and Applied Optics* **9**, pp. S196–S203, 2007.
5. A. A. M. Bui, A. B. Stilgoe, T. A. Nieminen, and H. Rubinsztein-Dunlop, "Calibration of nonspherical particles in optical tweezers using only position measurement," *Optics Letters* **38**(8), pp. 1244–1246, 2013.